Membrane-Dependent Modulation of the mTOR Activator Rheb: NMR Observations of a GTPase Tethered to a Lipid-Bilayer Nanodisc

Mohammad T. Mazhab-Jafari,[†] Christopher B. Marshall,[†] Peter B. Stathopulos,[†] Yoshihiro Kobashigawa,[‡] Vuk Stambolic,[†] Lewis E. Kay,[||,⊥] Fuyuhiko Inagaki,[‡] and Mitsuhiko Ikura*,[†]

[†]Department of Medical Biophysics, Campbell Family Cancer Research Institute, Ontario Cancer Institute, Princess Margaret Cancer Center, University Health Network, University of Toronto, Toronto, Ontario M5G 2M9, Canada
[‡]Faculty of Advanced Life Science, Hokkaido University, Sapporo 001-0021, Japan
[||]Departments of Molecular Genetics, Biochemistry, and Chemistry, University of Toronto, Toronto, Ontario M5S 1A8, Canada
[⊥]Program in Molecular Structure and Function, Hospital for Sick Children, Toronto, Ontario M5G 1X8, Canada

S *Supporting Information*

ABSTRACT: Like most Ras superfamily proteins, the GTPase domain of Ras homologue enriched in brain (Rheb) is tethered to cellular membranes through a prenylated cysteine in a flexible C-terminal region; however, little is known about how Rheb or other GTPases interact with the membrane or how this environment may affect their GTPase functions. We used NMR methods to characterize Rheb tethered to nanodiscs, monodisperse protein-encapsulated lipid bilayers with a diameter of 10 nm. Membrane conjugation markedly reduced the rate of intrinsic nucleotide exchange, while GTP hydrolysis was unchanged. NMR measurements revealed that the GTPase domain interacts transiently with the surface of the bilayer in two distinct preferred orientations, which are determined by the bound nucleotide. We propose models of membrane-dependent signal regulation by Rheb that shed light on previously unexplained in vivo properties of this GTPase. The study presented provides a general approach for direct experimental investigation of membrane-dependent properties of other Ras-superfamily GTPases.

Most Ras superfamily small GTPase proteins are targeted by prenylation to cellular membranes, where they function as switches in a variety of signaling networks. Following prenylation of a CaaX-box Cysteine residue (C; a is an aliphatic residue; X is the C-terminal amino acid) in the C-terminal hypervariable region (HVR),[1] the aaX peptide is cleaved by C-terminal prenylprotein peptidases, and Cys is carboxymethylated. Blockage of these post-translational modifications prevents GTPase-mediated signal transduction, highlighting the critical role of membrane localization. Hence, farnesyltransferase inhibitors have been developed to inhibit the biological activity of oncogenic Ras mutants.[2] While fluorescence-studies and molecular dynamic (MD) simulations have provided insight into small GTPase interactions with bilayer membranes,[3−6] atomic scale pictures of small GTPases on membranes are lacking due to the inherent challenges imposed by bilayer-membrane systems to high-resolution structural biology techniques.

Recent advances in the assembly of stable nanoscale bilayer membranes have made it possible to study structure, dynamics, and functions of peripheral and membrane-integrated proteins at the atomic level. Here, we used nanodiscs,[7] which are 5 × 10 nm discoidal lipoprotein complexes comprising a bilayer of 120−160 lipid molecules bounded and stabilized by two copies of an engineered variant of Apo-lipoprotein A,[8] to enable nuclear magnetic resonance (NMR)-based characterization of the structure, dynamics, and function of membrane-tethered Rheb. Rheb is targeted to endomembrane compartments including Golgi, endoplasmic reticulum and lysosomes via farnesylation of its sole Cys residue (Cys181), processing that is required for its activation of mTORC1.[9] To mimic processed Rheb, a truncated construct (residues 1−181) was covalently linked through Cys181 to a maleimide-conjugated lipid[6] incorporated into assembled nanodiscs (Figure 1A,B) or vesicles, a strategy previously described in studies of H-Ras on unilamellar vesicles.[6] Relative to vesicles, for which diameters of 20−500 nm are typical, the smaller size of nanodiscs results in rapid tumbling, enabling high-resolution NMR studies of membrane-anchored Rheb and NMR-based real-time assays[10] of the GTPase cycle of Rheb on the bilayer membrane.

Tethering Rheb to the nanodisc did not alter the rate of intrinsic GTP hydrolysis or the GTPase activating protein (GAP) TSC2-catalyzed GTP hydrolysis rates by Rheb (Figure 1C); however, the intrinsic nucleotide exchange rate was significantly reduced upon membrane association (Figure 1D), indicating that membrane conjugation directly impacts the GTPase cycle of Rheb. To investigate the structural and dynamical properties of the interactions between the membrane and the GTPase domain of tethered Rheb, we used chemical shift perturbation (CSP) analysis, ^{15}N R1, ^{15}N R2, steady-state ^{1}H−^{15}N NOE backbone relaxation measurements, and paramagnetic relaxation enhancement (PRE) experiments.

Conjugation of Rheb to the membrane did not detectably perturb the chemical shifts of resonances in the ^{1}H−^{15}N HSQC spectrum, with the exception of Cys181 (Figure S1), suggesting that the GTPase domain (1−169) and the HVR (170−180) of Rheb do not tightly associate with the bilayer. The overall
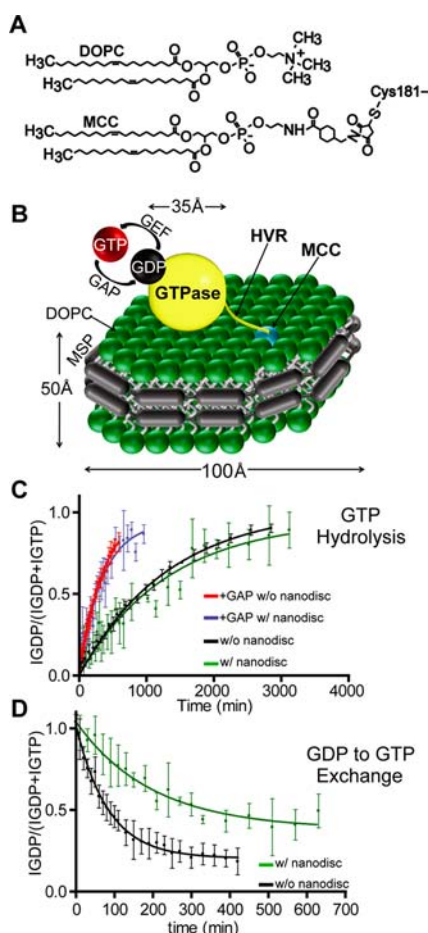
Figure 1. Tethering Rheb to a bilayer membrane inhibits nucleotide exchange and activation. (A) Lipids used for nanodisc assembly (full names in text). Reaction between Rheb Cys181 and the maleimide-moiety of PE-MCC was used to tether Rheb to the nanodisc bilayer. Drawn with ChemSketch (Advanced Chemistry Development, Inc.) (B) Schematic diagram of the Rheb-nanodisc complex. (C and D) Nucleotide hydrolysis and exchange reactions were monitored using NMR-based real-time GTPase assays of Rheb free in solution or tethered to nanodisc membrane bilayers. (C) Intrinsic GTP hydrolysis by free and nanodisc-bound Rheb are shown in black and green, respectively. GTP hydrolysis by free and nanodisc-bound Rheb in the presence of extract of HEK-293 cells overexpressing TSC1/TSC2 are shown in red and blue, respectively. (D) Intrinsic nucleotide exchange for free and nanodisc-bound Rheb are shown in black and green, respectively. I(GDP) and I(GTP) are intensities of several peaks in HSQC spectra that are specific to Rheb-GDP and -GTP, respectively. The higher plateau of the green curve reflects the greater impact of GTP hydrolysis when nucleotide exchange is slow.

rotational correlation time (τ_M) was calculated from ^{15}N R1, ^{15}N R2, and steady-state $^1H–^{15}N$ NOE[11] for GDP- and GMPPNP-(nonhydrolyzable analog of GTP) bound Rheb conjugated to the nanodisc and free in solution. Overall tumbling-times (τ_M) for Rheb-GDP were calculated to be 17.0 ± 0.2 ns in solution and 35.4 ± 1.3 ns when conjugated to the nanodiscs (20 °C). A protein rigidly associated with the >100 kDa Rheb-nanodisc complex would have an expected τ_M >60 ns (based on Stoke's law assuming a spherical protein-nanodisc complex); thus, the intermediate τ_M value indicates that the GTPase domain of Rheb-GDP exhibits a high degree of freedom (dynamics) despite being tethered to the membrane. The τ_M values for Rheb-GMPPNP in solution and conjugated to nanodiscs were 17.0 ±

0.5 and 32.6 ± 1.4 ns, respectively, similar to what was observed for Rheb-GDP. These results further establish the transient nature of Rheb's interactions with the membrane.

The most significant local changes in dynamics upon membrane binding were at the C-terminal HVR, where the backbone ps−ns motions were partially quenched, independent of the bound nucleotide (Figures S2, S3). Within the GTPase domain, the only significant change in local dynamics upon membrane conjugation was an increase in the μs−ms timescale motions in the α3 helix (R2 and R1 × R2 of residues 90−95) of Rheb-GDP, which was not observed for the GMPPNP-bound form (Figures S2, S3). The α3 helix forms ionic contacts with switch II in Rheb, and in the homologue H-Ras, α3 is allosterically coupled to the nucleotide binding site (NBS);[12] thus, the effect of membrane conjugation on the rate of nucleotide exchange may involve modulation of the NBS by perturbation of α3 dynamics. Another factor that might impair nucleotide exchange is occlusion of the NBS by the membrane surface; thus, we explored this possibility more fully by performing PRE experiments as detailed below.

The PRE effect can be powerful for identifying transient interactions, such as those between Rheb and the bilayer plane, and for determining "preferred conformations" of a protein such as membrane-associated Rheb. Rheb-tethered nanodiscs were prepared with the incorporation of lipids (5%) in which the headgroup was conjugated to the paramagnetic ion gadolinium (Gd^{3+}) (see Experimental Procedures in Supporting Information (SI)). Intensities of Rheb resonances were compared in the presence and absence of Gd^{3+} to identify specific residues that interact with the membrane (Figure 2A). For Rheb-GDP the residues broadened by the paramagnetic ion (defined as >50% decrease in peak intensity) were distributed throughout the GTPase domain (30 peaks), including the N-terminus, β2-β3 loop, C-terminus of switch II, C-terminus of α3 and, as expected, the HVR (11 peaks). Mapping these regions to the Rheb-GDP structure illuminates a patch surrounding residue 171, which links the GTPase domain to the HVR, which is prenylated in cells (Figure 2B).[13] The unusually slow rate of GTP hydrolysis by Rheb[10] allowed us to extend this PRE approach to Rheb bound to native GTP. The perturbed residues (24 in the GTPase-domain and 11 in the HVR) form a pattern similar to that seen for Rheb-GDP; however, the C-terminus of switch II was less broadened in the GTP-bound form, as was the C-terminus of α3, albeit with smaller differences here (Figure 2B). To generate atomic-resolution models of the Rheb-membrane complex, we performed simulations with High Ambiguity Driven biomolecular DOCKing (HADDOCK)[14] using our experimentally derived PRE-restraints (as described in Experimental Procedures in SI).

We generated 3000 models of Rheb docked to the membrane surface and the 300 models with lowest HADDOCK scores (a weighted sum of energy terms related to the interface and the individual components comprising the complex) were selected for cluster analysis. These models were grouped into clusters based on the orientation of Rheb relative to the membrane surface (i.e., RMSD following translation in the plane of the nanodisc and rotation about the normal axis, see experimental procedures in SI). Notably, mapping the PRE-affected residues on the structure of Rheb (Figures 2B, S5) illustrates that a single Rheb orientation cannot simultaneously satisfy all of the PRE-derived restraints, and indeed, two major clusters of solutions were identified for the GDP-bound form (Figures S4A, S5A). Cluster 1 (backbone RMSD cutoff = 8 Å) was oriented such that
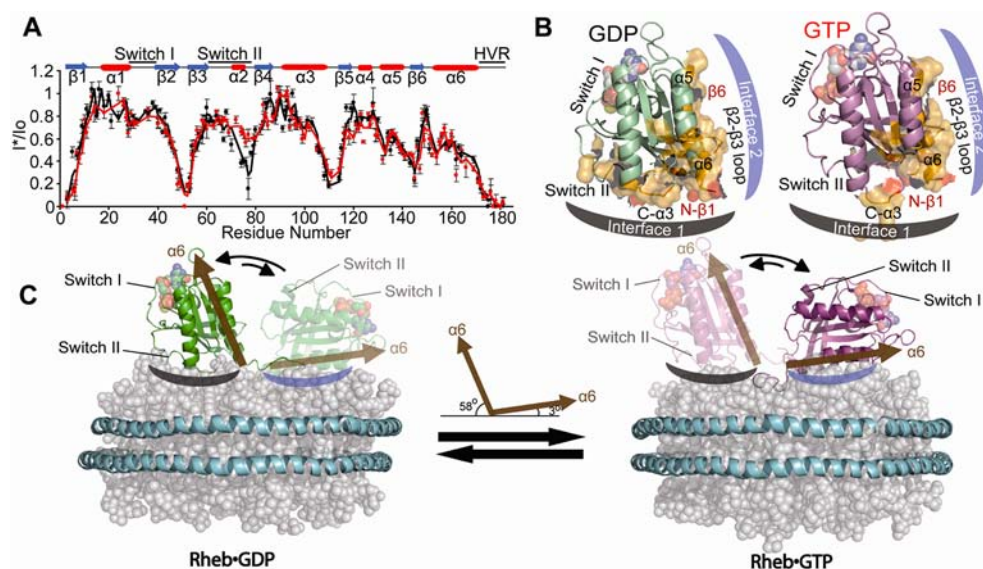
Figure 2. Identification of the Rheb-membrane interface and its modulation by the bound nucleotide. (A) Paramagnetic relaxation enhancement (PRE) of Rheb H(^{15}N) peak intensities induced by Gd^{3+}-conjugated lipids incorporated into nanodiscs. PRE effects detected for each residue of Rheb-GDP (black) and Rheb-GTP (red) presented as a ratio of H(^{15}N) resonance intensities of Rheb conjugated to nanodiscs in the presence (I*) or absence (Io) of Gd^{3+}. Error bars based on spectral noise. (B) PRE-affected residues mapped on Rheb G-domain. Residues that exhibited >50% and >80% peak broadening in the presence of Gd^{3+} are shown as orange and red surfaces, respectively, for Rheb-GDP (left) and -GTP (right), and two interfaces are identified. (C) PRE-driven HADDOCK models of Rheb-nanodisc complexes. Cluster center models of GDP- (left) and GTP- (right) bound Rheb in the semiperpendicular and semiparallel orientations. The nontransparent models reflect the favored conformation in each nucleotide bound state. The axis of Rheb α6 helix is shown with a brown arrow. PDB 1XTQ and 1XTS[15] were used in the calculations, and results were deposited as 2M4A and 2M4B for GDP- and GTP-bound states, respectively. PDBs of the complexes are also available by request.

the α6 helix (residues 153−171) was semiperpendicular (58° relative to the bilayer plane for the cluster center, i.e., model with the lowest RMSD to all other models within the cluster), while cluster 2 (backbone RMSD cutoff = 8 Å) was semiparallel (6° relative to the bilayer plane). Cluster 1 represented ~52% of the final solutions for Rheb·GDP docked to nanodiscs, while cluster 2 represented ~17% of the solutions. The remainder of the solutions formed small clusters, each of which comprised <10% of total solutions, or did not cluster. In both cluster 1 and 2 models, the NBS, comprising the P-loop, switch I, G4 (residues 118−123), and G5 (residues 149−151) boxes were facing away from the membrane bilayer and were >10 Å away (Figure S5A), consistent with the lack of broadening of these resonances, while the N-terminus, β2-β3 loop, and HVR were each within 10 Å of the bilayer plane. The major difference between the models in clusters 1 versus 2 was the reorientation of the G-domain with respect to the bilayer due to rotation about residue 171. This reorientation causes the C-terminal regions of switch II and α3 to sample positions proximal to the bilayer plane (<5 Å) in cluster 1, and distal from the bilayer plane (>10 Å) in cluster 2. The reorientation also brought α5 and β6 (residues 132−148) to within 10 Å of the bilayer in cluster 2. Likewise, two major clusters of models were identified for docking of 'activated' Rheb-GTP to the nanodisc (Figures S4B, S5B), with orientations similar to those determined for Rheb-GDP (i.e., cluster 1 exhibited a semiperpendicular orientation with an α6 angle of 54°, and cluster 2 was semiparallel with an α6 angle of 3°). Interestingly, relative to its GDP-counterpart, clusters 1 and 2 were more equally populated for Rheb-GTP, where 39 and 35% of total models were found in clusters 1 and 2, respectively. The relative cluster sizes were independent of the overall number of models calculated and were consistently reproducible. It is intriguing that on the basis of FRET analysis and MD simulations, remarkably similar semiperpendicular and semi-

parallel orientations have been proposed for H-Ras-GDP and -GTP interactions with the membrane, respectively.[3,4]

Our calculations show that the measured PRE restraints are consistent with an equilibrium between two distinguishable Rheb configurations, and that both of these conformers are populated by each of the GDP- and GTP-bound states, as illustrated in Figure 2C. The C-terminus of switch II of Rheb-GTP (residues 74−79) is significantly less perturbed by the PRE-tagged lipid than that of Rheb-GDP (Figure 2A), whereas the magnitude and distribution of the PRE effects are otherwise similar for both states; thus, the population of each clustered orientation is largely dictated by the nucleotide-specific PRE differences in switch II.

The low τ_M value we determined for membrane-tethered Rheb indicates considerable mobility on the membrane, most likely reflecting the fact that both semiperpendicular and semiparallel orientations are sampled during transient interactions between Rheb and the membrane surface. However, the semiperpendicular configuration 1 appears to be less favored in the GTP-bound state, due to subtle redistribution of surface electrostatics. The surface of the switch II-α3 region that forms the membrane interface in orientation 1 becomes less positively charged in the GTP-bound structure (Figure S6), which may diminish interactions with exposed negative charges in the phosphocholine bilayer.[16] Concomitantly, the α5-β6 of interface 2 becomes more positive in the GTP-bound structure, stabilizing the semiparallel orientation (Figure S6). Consistent with this notion, a GDP/GTP-dependent shift in the equilibrium between perpendicular and parallel orientations has been described for H-Ras-membrane interactions by MD simulations.[3,4] The NBS is not sterically occluded by the membrane surface in either perpendicular or parallel orientations; thus, we suggest that the mechanism by which membrane association impairs nucleotide exchange likely involves allosteric effects mediated via the membrane interaction, propagated from helix α3. The lower

kinetic rate indicates a higher activation energy for the rate-limiting step in the intrinsic exchange reaction, suggesting that the proposed allosteric effect might stabilize the NBS in the GDP-bound state.

Avruch and colleagues previously performed a comprehensive Ala-mutation scan of surface accessible residues in Rheb and analyzed their effects on cellular mTORC1 signaling.[17] Ectopic expression of Rheb with mutations in the C-terminal region of switch II that did not impair GTP binding, nevertheless abolished the rescue of mTORC1 signaling in nutrient starved cells, and relative to wild-type Rheb, significantly reduced mTORC1 output in replenished cells with endogenous Rheb knocked down. This phenotype is similar to that observed with the nucleotide-deficient Rheb mutant D60I, but appears to be mediated by a different mechanism.[18] Our data show that the C-terminal residues of switch II form part of the Rheb-membrane interface in cluster 1 of the GDP and GTP-bound states, but become solvent exposed in cluster 2. In light of these observations, we propose that the membrane acts as a regulatory platform in Rheb-mTORC1 communication in cells, in synergy with the GTPase cycle of Rheb. In our proposed model, the nucleotide-dependent reorientation of Rheb regulates communication with mTORC1 in cells by GTP-mediated exposure of switch II. A similar mode of GTPase-effector regulation has been suggested for H-Ras interactions with the Ras binding domain (RBD) of C-Raf and Phosphatidylinositol 3-kinase γ (PI3Kγ).[19] However, as the Rheb-binding domain in mTOR has not been defined, the precise molecular details of mTORC1 regulation by the C-terminal switch II segment of Rheb in vivo remain to be fully elucidated.

Interestingly, a recent structure of Rheb in complex with PDEδ, a nucleotide-independent guanine dissociation inhibitor (GDI)-like protein,[20] reveals that PDEδ captures the farnesyl tail of Rheb in a deep pocket, and makes additional contacts (~20% of the total buried surface area) with the N-terminal β1 strand, and to a lesser extent, the C-terminal loop of switch II. Thus, overlaying the Rheb-PDEδ structure with Rheb-nanodisc models 1 and 2, it is evident that steric clashes between PDEδ and the membrane bilayer would preclude the Rheb-PDEδ complex from adopting a model 1 orientation, and likewise block PDEδ from binding this state of Rheb (Figure S7A). However, because of the transient nature of the Rheb-membrane interaction, other orientations sampled by the G-domain of Rheb including model 2 would allow the β1 strand and the C-terminal loop of switch II to interact with PDEδ (Figure S7B). Formation of this complex would then restrict G-domain interactions with the membrane and may initiate solubilization of Rheb, involving extraction of the farnesyl moiety from the bilayer into the hydrophobic pocket of PDEδ.

To our knowledge, the present study is the first experimental work to directly probe membrane-dependent regulation of the structure and function of a GTPase at atomic resolution, and provides a general approach for direct experimental studies on membrane-dependent regulation of other GTPases.

ASSOCIATED CONTENT

Ⓢ Supporting Information

Supplementary methods and figures. This material is available free of charge via the Internet at http://pubs.acs.org.

AUTHOR INFORMATION

Corresponding Author

mikura@uhnres.utoronto.ca

REFERENCES

(1) Brunsveld, L.; Waldmann, H.; Huster, D. *Biochim. Biophys. Acta* **2009**, *1788*, 273.
(2) Berndt, N.; Hamilton, A. D.; Sebti, S. M. *Nat. Rev. Cancer* **2011**, *11*, 775.
(3) Abankwa, D.; Hanzal-Bayer, M.; Ariotti, N.; Plowman, S. J.; Gorfe, A. A.; Parton, R. G.; McCammon, J. A.; Hancock, J. F. *Embo J.* **2008**, *27*, 727.
(4) Gorfe, A. A.; Hanzal-Bayer, M.; Abankwa, D.; Hancock, J. F.; McCammon, J. A. *J. Med. Chem.* **2007**, *50*, 674.
(5) Gorfe, A. A.; Babakhani, A.; McCammon, J. A. *J. Am. Chem. Soc.* **2007**, *129*, 12280.
(6) Gureasko, J.; Galush, W. J.; Boykevisch, S.; Sondermann, H.; Bar-Sagi, D.; Groves, J. T.; Kuriyan, J. *Nat. Struct. Mol. Biol.* **2008**, *15*, 452.
(7) Ritchie, T. K.; G., Y.; Bayburt, T. H.; Denisov, I. G.; Zolnerciks, J. K.; Atkins, W. M.; Sligar, S. G. *Methods Enzymol.* **2009**, *464*, 211.
(8) Denisov, I. G.; Grinkova, Y. V.; Lazarides, A. A.; Sligar, S. G. *J. Am. Chem. Soc.* **2004**, *126*, 3477.
(9) Buerger, C.; DeVries, B.; Stambolic, V. *Biochem. Biophys. Res. Commun.* **2006**, *344*, 869.
(10) Marshall, C. B.; Ho, J.; Buerger, C.; Plevin, M. J.; Li, G. Y.; Li, Z.; Ikura, M.; Stambolic, V. *Sci. Signaling* **2009**, *2*, ra3.
(11) Farrow, N. A.; Z., O.; Szabo, A.; Torchia, D. A.; Kay, L. E. *J. Biomol. NMR.* **1995**, *6*, 153.
(12) Fraser, J. S.; van den Bedem, H.; Samelson, A. J.; Lang, P. T.; Holton, J. M.; Echols, N.; Alber, T. *Proc. Natl. Acad. Sci. U.S.A.* **2011**, *108*, 16247.
(13) Clark, G. J.; Kinch, M. S.; Rogers-Graham, K.; Sebti, S. M.; Hamilton, A. D.; Der, C. J. *J. Biol. Chem.* **1997**, *272*, 10608.
(14) Dominguez, C.; Boelens, R.; Bonvin, A. M. *J. Am. Chem. Soc.* **2003**, *125*, 1731.
(15) Yu, Y.; Li, S.; Xu, X.; Li, Y.; Guan, K.; Arnold, E.; Ding, J. *J. Biol. Chem.* **2005**, *280*, 17093.
(16) Semchyschyn, D. J.; Macdonald, P. M. *Magn. Reson. Chem.* **2004**, *42*, 89.
(17) Long, X.; Lin, Y.; Ortiz-Vega, S.; Busch, S.; Avruch, J. *J. Biol. Chem.* **2007**, *282*, 18542.
(18) Tabancay, A. P., Jr.; Gau, C. L.; Machado, I. M.; Uhlmann, E. J.; Gutmann, D. H.; Guo, L.; Tamanoi, F. *J. Biol. Chem.* **2003**, *278*, 39921.
(19) Abankwa, D.; Gorfe, A. A.; Hancock, J. F. *Cell Cycle* **2008**, *7*, 2667.
(20) Ismail, S. A.; Chen, Y. X.; Rusinova, A.; Chandra, A.; Bierbaum, M.; Gremer, L.; Triola, G.; Waldmann, H.; Bastiaens, P. I.; Wittinghofer, A. *Nat. Chem. Biol.* **2011**, *7*, 942.